Title

Relative density effects on the bearing capacity of unsaturated sand

Journal

Soils and Foundations, 59(5)

ISSN

0038-0806

Authors

Vaseghi Maghvan, Sajjad
Imam, Reza
McCartney, John S

Publication Date

2019-10-01

DOI

10.1016/j.sandf.2019.05.011

Peer reviewed

Elsevier Editorial System(tm) for Soils and Foundations

Manuscript Draft

Manuscript Number: SANDF-D-18-00188R2

Title: RELATIVE DENSITY EFFECTS ON THE BEARING CAPACITY OF UNSATURATED SAND

Article Type: Technical Paper

Keywords: Bearing Capacity, Unsaturated Soil, Relative Density, Matric Suction, shear strength, SWRC.

Corresponding Author: Professor Reza Imam, Ph.D.

Corresponding Author's Institution:

First Author: Sajjad Vaseghi Maghvan, MSc.

Order of Authors: Sajjad Vaseghi Maghvan, MSc.; Reza Imam, Ph.D.; John S McCartney, PhD

Abstract: This study focuses on the impact of relative density on the bearing capacity of unsaturated sand using both theoretical predictions and measurements from physical modeling tests. The theoretical predictions incorporate the effective stress, quantified using the suction stress concept and friction angles obtained from direct shear tests on unsaturated sand specimens at different relative densities and degrees of saturation, into conventional bearing capacity equations. The suction stress values inferred from the failure envelopes were found to match well with values predicted from the soil-water retention curves for sands with different relative densities. Moreover, the bearing capacity values measured in physical modeling experiments involving loading of a circular footing atop unsaturated silty sand layers having different initial degrees of saturation matched well with the predicted bearing capacity values from an effective-stress based model. As expected, the bearing capacity was greater for soils with increasing relative density, but an interesting observation is that a transition from general to local shear failure occurred at a certain combination of relative density and degree of saturation. For the silty sand tested, this transition occurred at a relative density of 0% for degrees of saturation between 4 and 16% and at a relative density of 40% for degrees of saturation between 30 and 90%. General shear failure was always observed at relative densities of 70 and 90%.

RELATIVE DENSITY EFFECTS ON THE BEARING CAPACITY OF UNSATURATED SAND

Sajjad Vaseghi Maghvan[1], Reza Imam[2], John S. McCartney[3]

ABSTRACT: This study focuses on the impact of relative density on the bearing capacity of unsaturated sand using both theoretical predictions and measurements from physical modeling tests. The theoretical predictions incorporate the effective stress, quantified using the suction stress concept and friction angles obtained from direct shear tests on unsaturated sand specimens at different relative densities and degrees of saturation, into conventional bearing capacity equations. The suction stress values inferred from the failure envelopes were found to match well with values predicted from the soil-water retention curves for sands with different relative densities. Moreover, the bearing capacity values measured in physical modeling experiments involving loading of a circular footing atop unsaturated silty sand layers having different initial degrees of saturation matched well with the predicted bearing capacity values from an effective-stress based model. As expected, the bearing capacity was greater for soils with increasing relative density, but an interesting observation is that a transition from general to local shear failure occurred at a certain combination of relative density and degree of saturation. For the silty sand tested, this transition occurred at a relative density of 0% for degrees of saturation between 4 and 16% and at a relative density of 40% for degrees of saturation between 30 and 90%. General shear failure was always observed at relative densities of 70 and 90%.

[1] Lecturer, Amirkabir University of Technology, Dept. of Civil and Environmental Engineering, Tehran, Iran, 0098 91 4530 7488, svmagvan-sf69@aut.ac.ir.

[2] Assistant Professor and Head of Geotechnical Engineering Group, (Corresponding Author), Amirkabir University of Technology, Dept. of Civil and Environmental Engineering, Tehran, Iran, 0098 21 6454 3040, rimam@aut.ac.ir.

[3] Professor and Department Chair, University of California San Diego, Dept. of Structural Engineering. 9500 Gilman Dr., La Jolla, CA 92093-0085, mccartney@ucsd.edu.

KEYWORDS: Bearing Capacity, Unsaturated Soil, Relative Density, SWRC, Suction Stress.

INTRODUCTION

It is common in geotechnical practice to estimate the bearing capacity and settlement of shallow foundations without accounting for the effects of soil degree of saturation and matric suction. (Oh and Vanapalli, 2011; Oh et al., 2009). However, these simplifying assumptions may lead to uneconomical foundation designs (Steensen Bach et al. 1987, Vanapalli and Mohamed, 2007; Uchaipichant, 2010). Although it is typically assumed that saturated soils provide a worst-case scenario with regards to shear strength, bearing capacity, and settlement, this assumption may not represent the realistic setting for many shallow foundations and may not be valid for failure back-analyses. In some cases, the soil beneath shallow foundations may remain in unsaturated conditions through the use of drainage systems and hydraulic barriers. Accordingly, it may be advantageous to consider the effects of unsaturated conditions on the bearing capacity of shallow foundations. Several studies have performed experiments and developed theories to measure and estimate the bearing capacity of shallow foundations on unsaturated soil layers, respectively, with the general conclusion that the bearing capacity increases with decreasing degree of saturation (Broms, 1965; Steensen-Bach et al., 1987; Fredlund and Rahardjo, 1993; Schnaid et al., 1995; Oloo et al., 1997; Miller and Muraleetharan, 1998; Sheng et al., 2003; Costa et al., 2003; Mohamed and Vanapalli, 2006; Vanapalli and Mohamed, 2007; Oh and Vanapalli, 2011; Vanapalli and Mohamed, 2013; Vahedifard and Robinson, 2016; Tang et al., 2016). However, the experimental investigations in these studies were restricted to a single or limited number of relative densities for a given soil type and/or did not consider a wide range of degrees of saturation. These two variables are expected to

have important effects on the effective stress state, as the relative density affects the shape of the soil-water retention curve (SWRC) and suction stress characteristic curve (SSCC) (Lu et al. 2010).

An additional reason to consider the combined effects of relative density and degree of saturation is that the failure mode of soils beneath shallow foundations depends on the combined effect of the shear strength of the soil, which is a function of the effective stress state and relative density, and the foundation boundary conditions (e.g., footing embedment depth). For very dense sands loaded by small footings, general failure is the predominant failure mode, whereas sand with loose to medium density experience a punching or local shearing failure mode, respectively such that the values of bearing capacity are close to those obtained in the case of constant critical friction angle and no dilatancy (Simonini, 1993; Oh and Vanapalli, 2011). The interaction between the unsaturated conditions and relative density may lead to changes in the failure mode, adding further complexity to the shallow footing bearing capacity problem. Although Perkins and Madson (2000) observed that transitions in the failure modes of the soil under shallow footings (i.e., transition from local shearing to general shearing) may occur with increase in relative density, the role of unsaturated conditions on these transitions has not been investigated, and the interplay between relative density and unsaturated conditions is not well understood. It is expected that unsaturated conditions may have some effect on the transition in bearing capacity failure modes as Bolton (1986); Simonini (1993); and Loukidids and Salgado (2011) found that the internal friction angle, ϕ, and dilatancy angle of different sands are affected by both the relative density and the mean effective stress. The mean effective stress in unsaturated soils in turn depends on the suction stress, which is a

function of the degree of saturation and matric suction (Lu and Likos, 2004; Ciervo et al., 2015). Lu et al. (2010) found that the suction stress can be predicted from the SWRC. Imam et al. (2018) investigated the impact of relative density on the SWRC, SSCC, and shear strength of an unsaturated silty sand and found that increases in relative density led to increases in the peak shear strength, as expected, but the maximum suction stress occurred at lower degrees of saturation for denser soils.

The main goal of this study is to investigate the impact of relative density on the shear strength and bearing capacity of unsaturated sand through a series of direct shear tests and physical modeling tests involving loading of surface footings on unsaturated sand layers. These unsaturated sand layers were prepared with different relative densities and initial degrees of saturation to identify potential transition points in the bearing capacity failure mode.

EXPERIMENTAL PROGRAM

Materials

A fine-grained silty sand classified as SP-SM according to the Unified Soil Classification Scheme (USCS) was used in this study. The grain size distribution for the soil is shown in Figure 1, and some of its basic physical properties are provided in Table 1. The mean grain size of the tested soil (i.e., D_{50}) is 0.135 mm, so it is not expected that there will be a particle size effect on the results of the physical modeling tests. Specifically, the ratio of the footing with D to the mean grain size (D/D_{50}) used in the footing loading tests is 746, which is much greater than the minimum ratio required for the elimination of possible particle size effects (Lau and Bolton 2011). Although the soil contains silt-sized fines, no evidence of a bimodal pore size distribution was observed in the grain size distribution or other tests. Accordingly, the presence of the silt-

sized fines does not lead to a bimodal SWRC or associated effects on the shear strength (Ciervo et al., 2015). The standard Proctor compaction curve for the sand is shown in Figure 2. The compaction curve is relatively flat with a variation in unit weight of 5% for the different water contents.

Direct Shear Tests

Direct shear tests with a 100 mm × 100 mm × 30 mm box under initial vertical stresses of 50, 100, and 200 kPa were conducted on specimens of the silty sand at seven different initial degrees of saturation of 0, 4, 16, 30, 60, 90 and 100%. After mixing the soil with water to reach a given target gravimetric water content, the moist soil was kept in airtight bags for 24 hours to reach moisture equilibrium. The soil specimens were then formed in the direct shear box using moist tamping to reach the desired initial relative densities of 0, 40, 70, and 90% at the different initial degrees of saturation mentioned above. The loosest specimens were prepared by carefully leveling the soil in a single lift without the need for tamping, but the denser specimens required tamping of 3 lifts with a 10 mm-diameter rod. As the amount of tamping needed to reach a certain density changed with each specimen, it was not possible to quantify the compaction energy used to prepare the specimens, but it was possible to reach consistent relative densities by monitoring the specimen height and soil mass. A possible shortcoming of using this specimen preparation technique to evaluate the effects of the initial degree of saturation is possible differences in soil structure for the specimens having a similar relative density but different degrees of saturation. For example, Mitchell et al. (1965) found that compacting fine-grained soils at different water contents led to changes in engineering properties and attributed this to changes in soil structure. Such changes in clayey soils may be

caused by differences in: the degree of particle flocculation and dispersion (Lambe and Whitman, 1979), the formation and distribution of micro- and macro-pores changing the in SWRC (Birle et al., 2008), etc. In the case of sandy soils, past studies e.g., Ishihara and Verdugo, 1996; Wood et al., 2008) have shown that different methods of sample preparation such as moist tamping, dry deposition, water sedimentation, etc. can lead to different structures. Ishihara and Verdugo (1996) showed that this results in different stress-strain behaviors at smaller strains, but the same strength due to the possible elimination of soil structure at large strain. Wood et al. (2008) concluded that the behavior of denser silty sand is not affected by the sample preparation method but that these effects increase with silt content. As indicated previously, in the current study, the soil tested contains 7% non-plastic (rock flour) fines and all samples tested were prepared using only the method of moist tamping to minimize possible differences in structure caused by the method of sample preparation.

Shear stresses were applied to the direct shear test specimens in a displacement-controlled manner with a rate of 1 mm/min under constant water content conditions. Area corrections were applied in calculating both the vertical and shear stresses during shearing. Changes in the degree of saturation during shearing assessed by measuring the gravimetric water content at the beginning and end of the tests were found to be negligible (a maximum change of less than 1 to 3% of the initial degree of saturation). During shearing no water outflow was observed even for the specimens with S=90%, confirming the constant water content condition. Therefore, the initial degree of saturation was used to interpret the shear strength values at failure. Further, as the degree of saturation did not change significantly during shearing, it can be assumed that suction changes are negligible for this soil during

constant water content shearing. More details are provided by Imam et al. (2018). The displacement at the point of shear failure in the experiments was defined as that corresponding to the peak value of the mobilized secant friction angle. The shear stress values from the plots of shear strength vs. horizontal displacement at these displacements were then selected as the shear strengths for the various relative density and degrees of saturation, an approach similar to that used by Ghaaowd et al. (2017) and Imam et al. (2018). Imam et al. (2018) reported the stress-strain curves for the tests in this study, which indicate that the specimens with a relative density of 0% always show contraction during shearing, the specimens with a relative density of 40% show contraction for higher normal stresses and dilation for lower normal stresses, while the specimens with relative densities of 70 and 90% always show dilation during shearing. The dilations observed in the direct shear tests may not be the same as those observed in the tank tests due to the different constraints on particle movement, which may lead to a source of uncertainty when using the friction angles from the direct shear tests to predict the bearing capacity from the tank tests. Nonetheless, the direct shear tests are useful to reveal that the transitional behavior in the dilatancy can be expected around a relative density of 40%.

Linear failure envelopes based on the net vertical stress for the soil at relative densities of 0, 40, 70, and 90% and different initial degrees of saturation are shown in Figure 3(a). Properties of the soil at these relative densities are also shown in Table 2. Values of the drained friction angles and apparent cohesion along with the coefficients of determination, R^2, for the different failure envelopes obtained from Figure 3(a) are listed in Table 3. The effective friction angle for the specimens at each relative density does not change significantly with the initial degree of saturation, while the apparent cohesion, determined as the ordinate intercepts of the

failure envelopes, increased with decreasing initial degree of saturation. As expected, the effective friction angle derived from the peak shear strengths increases with increase in the soil relative density, minimum and maximum of which were 31.0° and 36.3° for the soil at relative densities of 0 and 90%, respectively. The shear strengths of sand having different initial relative densities of 0, 40, 70, and 90% is plotted as a function of the initial degree of saturation in Figure 3(b). A nonlinear change in shear strength with degree of saturation is observed.

The contact filter paper method was used for the determination of matric suction of the soil to define the SWRC. Since the soil used in the current study is coarse-grained with negligible osmotic suction, the contact filter paper method was used to measure the matric suction. The SWRC model of van Genuchten (1980) was fitted to the SWRC data, and is given as follows:

$$S_e = \left[\frac{1}{1 + \{\alpha_{vG}(u_a - u_w)\}^{n_{vG}}}\right]^{(1-1/n_{vG})} \quad (1)$$

where u_a is the pore air pressure, u_w is the pore water pressure, and the term $(u_a - u_w)$ is the matric suction. The terms α_{vG} and n_{vG} are fitting parameters, and S_e is the effective saturation defined as follows:

$$S_e = \frac{S_r - S_{res}}{1 - S_{res}} \quad (2)$$

where S_r is the degree of saturation and S_{res} is the residual saturation. The SWRC data along with the fitted SWRC of van Genuchten (1980) for the soil at four different relative densities of 0, 40, 70, and 90% are shown in Figure 4(a). The air-entry value (AEV), the degree of saturation at residual state (i.e., S_{res}) and the van Genuchten (1980) SWRC fitting parameters are summarized in Table 4. As the soil used in this study is granular, there is no inclination to form

aggregation, therefore the soil's structure is expected to display a monomodal pore size distribution (Zhao et al., 20; Casini et al., 2012). By using monomodal pore size distribution, Lu et al. (2010) presented a closed form relationship for the effective stress in unsaturated soils which can be intrinsically related to the SWRC as follows:

$$\sigma' = (\sigma - u_a) - \sigma^s \tag{3}$$

where σ' is the effective stress, σ is the total stress, and σ^s is the suction stress, defined as the product of the effective saturation and the matric suction (i.e., $S_e\{u_a - u_w\}$). This permits the SWRC model in Equation (1) to be integrated into the definition of the effective stress, as follows:

$$\sigma' = (\sigma - u_a) + \frac{S_e}{\alpha_{vG}}\left(S_e^{\frac{n_{vG}}{1-n_{vG}}} - 1\right)^{\frac{1}{n_{vG}}} \tag{4}$$

The Mohr-Coulomb failure criterion can be used to predict the impact of effective saturation on the shear strength of unsaturated soils in direct shear tests, as follows (Lu et al., 2010):

$$\tau_f = c' + \left[(\sigma - u_a) + \frac{S_e}{\alpha_{vG}}\left(S_e^{\frac{n_{vG}}{1-n_{vG}}} - 1\right)^{\frac{1}{n_{vG}}}\right]\tan\phi' \tag{5}$$

where τ_f is the shear stress at failure at a given effective saturation, c' is the drained cohesion (typically assumed to equal zero for uncemented granular soils), and ϕ' is the drained friction angle. Based on the results from the direct shear tests, the internal friction angle is assumed to not vary with the degree of saturation or matric suction (Bouazza et al., 2006; Oh et al., 2011).

Experimental values of suction stress were estimated from the shear strength values τ_f from the failure envelopes in Figure 3(a), as follows (Lu et al., 2010):

$$\sigma^s = -\frac{\tau_f - (\sigma - u_a)\tan\phi'}{\tan\phi'} \quad (6)$$

To use this equation, it is assumed that the value of c' is equal to zero and that the failure envelope is linear. Further, the value of $\tan\phi'$ for sand at a given relative density was assumed to not depend on the initial degree of saturation, as noted in the analysis of the data in Figure 3(a). The suction stress values estimated from Equation (6) using the failure envelopes from the direct shear test results are shown in Figure 4(b), along with the predicted suction stress values from the model of Lu et al. (2010) that incorporate the parameters of the SWRC in Figure 4(a). The match between the predicted and measured suction stress values is good for the specimens with relative densities of 0 and 40%, but greater discrepancies are noted for the specimens with relative densities of 70 and 90%. Nonetheless, the predicted suction stress characteristic curves capture both the increase in the suction stress with increasing relative density as well as the shift to the left observed in the data. Discrepancies in the magnitude of the predicted and experimental suction stress values noted at low degrees of saturation could be because the SWRC data does not follow the same shape as the fitted van Genuchten (1980) SWRC model at high suctions (low degrees of saturation). However, the SWRC models in Figure 4(a) represent the best fit to all of the SWRC data points over the full range of the degree of saturation. A curve connecting the maximum values of suction stresses obtained for various relative densities is also presented in Figure 4(b), referred to as the line of maximums. The maximum value of suction stress occurs at lower degrees of saturation for denser specimens. As observed in the SWRCs in Figure 4(a) and in the parameters listed in Table 3, the matric suction at AEV and at S_{res} increase with increase in the soil relative density. However, increases

in the relative density leads to deceases in both α_{vG} and n_{vG} since the former approximates the inverse of suction at the AEV and the latter is related to the pore size distribution, both of which decrease with increasing soil density (van Genuchten, 1980). Overall, the analysis in Figure 4 confirms that an effective stress analysis is appropriate for predicting shear strength of unsaturated soils and the interpretation of the behavior of shallow footings placed on unsaturated soil layers.

Physical Modeling Tests

While small-scale loading tests using footings on or in soil layers provide an opportunity to understand footing behavior in carefully-controlled laboratory conditions by comparing results between different tests, some considerations in terms of scaling effects should be considered when extending measurements from these small-scale tests to full-scale foundations. Previous studies have shown that scale effects are mainly due to differences between the model footing and the prototype with regards to: (i) the level of stress applied by the footing to subsoil, (ii) the ratio of footing width to soil grain size, (iii) the soil anisotropy and the resulting differences in the orientation of failure plane with respect to soil bedding plane, and (iv) the progressive failure and non-uniform strains developed in the soil along the failure surface (Lau and Bolton, 2011). In the case of footings resting on unsaturated soils, the difference in the footing size also leads to difference in the size of the influence zone under the footing that is subjected to increased stress due to footing load. Since the footing behavior depends on the matric suction in this zone, differences in size of this zone lead to differences in the average matric suction within this zone if the matric suction varies with depth (Oh and Vanapalli, 2013).

Based on past studies, the most important scale effect of those listed above is the difference in stress level between the model and the full-scale footings (see e. g. Lau and Bolton, 2011). Larger footings induce higher stresses in the influence zone and, due to non-linearity of the Mohr-Coulomb failure envelope (i.e. the higher friction angle at lower stresses), the friction angle mobilized at failure is larger in model footings compared to full-scale footings (De Beer, 1965). This stress-dependency is higher in denser sands due to the higher curvature of their failure envelope (Colliat-Dangus et al., 1988).

Several methods have been used successfully to account for scale effects of surface footings, allowing results of model tests to be generalized to full scale conditions with some of them relating bearing capacities of footings with ratios of dimensions of up to 100 (e.g. Zhu et al., 2001).They include: use of friction angles that are functions of the applied pressure in the determination of the bearing capacity factor $N\gamma$ (Lau and Bolton, 2011); plotting the applied stress versus the normalized settlement curves (i.e., settlement/dimension of footing, S/D) (Briaud and Gibbens, 1997; Palmer, 1948); use of values for N_γ that are functions of footing size (Zhu et al., 2001; Shiraishi, 1990); and, use of the state parameter concept to relate results from a certain combination of void ratio and mean stress to another combination (Cerato and Lutenegger, 2007).

Another factor that influences the bearing capacity is the ratio of the footing width, D (or footing diameter in circular footings) to mean grain size of the soil (i.e., D/D_{50}) (Herle, 1997). Kusakabe (1995) recommended physical model testing with D/D_{50} ranging from a minimum value of 50 to 100 to avoid the particle size effect. As noted in the materials section, particle size effects are not expected for the soil and foundation diameter selected.

Results of physical modeling of surface footings on unsaturated soil layers should also be interpreted considering the distribution of matric suction (or degree of saturation) with depth. In most cases, the average matric suction is used in calculations of the bearing capacity, settlement, modulus of elasticity, etc., when considering effects of the degree of saturation (e.g., Oh and Vanapalli, 2013; Vahedifard and Robinson, 2016; Vanapalli and Mohamed, 2007). The average matric suction may be a function of the footing dimension, since smaller footings will influence a smaller volume of soil beneath the footing and may have a different average matric suction than larger footings, if matric suction varies with depth. However, if the matric suction distribution profile with depth is uniform, the average matric suction will be the same regardless of footing size (Oh and Vanapalli, 2013).

The scaling issues indicated above were considered in conducting the physical model tests in this study. In this respect, particle size of the soil tested was selected such that the ratio of footing width to average soil particle size remains much greater than 200. Further, the soil layers were prepared with a uniform profile of the degree of saturation with depth such that the difference in footing size in the model and prototype would not result in different values for the average degree of saturation in the underlying soil layer.

Model tests were conducted on a circular footing consisting of an aluminum plate having a diameter of 100 mm and a thickness of 15 mm resting atop a silty sand soil placed in a square tank of 500 mm × 500 mm area and 1000 mm height, to investigate the effect of soil initial degree of saturation on the bearing capacity and load-settlement behavior of a silty sand soil at relative densities of 0, 40, 70, and 90%. These relative densities are categorized as loose, medium, dense, and very dense soil, respectively, such that results of the experiments would

be beneficial in the examination of the changes in the failure modes of the footing in various soil densities and degrees of saturation. In this respect, the possible transition from punching to local or from local to general shearing failure of the soil were examined. Details of the experimental setup and the accessories used for characterization of the axial loading response of the tested soil are shown in Figure 5.

For each test, the sand was mixed with the specified percentage of water to achieve each of the six target degrees of saturation of 0, 4, 16, 30, 60, and 90%. For the soil at relative densities of 70% and 90%, the soil layers were prepared only at degrees of saturation of 4, 16, and 60% since compacting the soil at higher degrees of saturation to relative densities of 70 and 90% was not so easy. Furthermore, it is expected that the behavior of more interest for the soil with relative densities of 70 and 90% occurs at lower degrees of saturation. The moist soil was placed in the tank in 50 mm-thick layers. The loosest specimens were prepared by leveling the loose soil, while the denser specimens were prepared by applying several blows of a hammer having a plastic head with a flat, 50 mm x 50 mm square face. The number of blows varied from specimen to specimen to achieve the specified relative densities. Parallel horizontal lines were drawn inside the test tank to control the compaction of each layer and reach the specified density. After placement of the soil layers, the soil surface was carefully leveled to provide a reference for any surface bulging. The water added to the soil at the time of mixing was slightly higher than the target value such that the desired initial (before loading) degree of saturation of the circular footing would be achieved due to evaporative losses occurring during mixing. The additional water added to compensate for subsequent losses so that the target initial degrees of saturation could be achieved was slightly higher for higher target degrees of

saturation. Although this process was not quantified, the achieved initial degrees of saturation after compaction were consistently equal to the target values. For the denser specimens, lower layers of the soil in the test tank were compacted with lower effort compared to the upper layers, knowing that the lower layers may densify when compacting the upper layers. Although the undercompaction technique was not followed strictly, the achieved relative densities were consistent in each tank test. In addition to tracking the thickness and mass of each lift during soil placement, the variations in the soil relative density with depth were confirmed after compaction for each test were determined using a cylindrical hollow tube having an inner diameter of 46 mm, thickness of 0.8 mm and length of 200 mm. The tube was pushed into the soil layers, and samples of unsaturated soil with a height of 50 mm were extracted at each step, and the soil was dried to determine its gravimetric water content and relative density, knowing the internal volume of the tube. The achieved relative densities are shown in Figure 6, which shows that the relative densities are consistent from test to test. Although a slight increasing trend in relative density with depth is noted, the soil in the upper region is very close to the target relative densities. This is important as this is the soil in this region will have the greatest effect on the surface footing response. Small differences for the soil layers compacted to relative densities of 70 and 90% were observed. Tests were performed on the soil layers 7 days after their compaction (to promote homogenization of water content) by measuring the load-settlement behavior of the circular footing placed on the surface of the soil layer loaded in a displacement-controlled manner at a rate of 1 mm/min. Knowing the area of the loading plate, the applied average pressure under the loading plate was calculated.

Care was taken to minimize evaporation from the soil layers between preparation and testing by covering the soil surface with plastic wrap. Although not shown, samples taken from the soil layers before loading showed negligible variations in the degree of saturation with depth. Further, the degree of saturation at the time of loading varied by less than 1-3% from the target value at soil placement. Accordingly, it is assumed that the profiles of the degree of saturation and matric suction in the soil layers in this zone are approximately uniform.

RESULTS

Stress-Settlement Curves and Bearing Capacity

The relationships between the applied stresses to the footing and its settlement at various initial degrees of saturation and four relative densities of 0 and 40, 70, and 90% are shown in Figure 7. The degrees of saturation shown in the figures are those measured for each test at the beginning of loading.

Failure Mechanism

Bearing capacity failure modes of footings placed on sand at various relative densities and depths have been studied extensively by Vesic (1963, 1973). The model footing tests of Vesic showed that a circular footing having 152 mm diameter placed on the surface of sandy soil exhibited three types of load (vertical axis) vs. settlement (horizontal axis) curves: (i) curves exhibiting a peak load followed by a post-peak drop, observed in footings placed on dense sand, and representing general shear failure with bulging of the soil around the footing (b) curves with constant or mildly decreasing slope observed in loose sand, representing punching shear failure and densification of the loose sand, with almost no bulging, and (c) curves with higher initial slope followed by a distinct smaller slope or a near flat (zero slope) portion, representing

local shear failure, that may be associated with limited bulging. Subsequent studies on the effect of sand density and footing depth on the failure mode (Vesic, 1973) showed that for the test conditions studied, model footings placed on sand surface exhibited general shear failure when sand relative densities varied from about 72% to 100%, local shear failure for relative densities of about 35% to 72% and punching shear failure for relative densities of 0% to about 35%.

Based on the studies described before, it is expected that for the soil at relative densities of 0% and 40%, punching and local shear failure mechanisms may develop, respectively (Vesić, 1973). However, Figure 7 shows that while these expected modes may occur for soils at degrees of saturation of 0% to 4% and for 60% to 90%, an examination of the shapes of the load-settlement curves indicates that failure modes typically attributed to denser soils may be observed in looser soils under some degrees of saturation. In unsaturated soils, the failure mode is also affected by the degree of saturation in addition to the relative density, although scale effects may also play a role. The results in Figures 7(c) and 7(d) also show that the load-settlement behavior of soils at relative densities of 70% and 90% is representative of general shear failure for all degrees of saturation, as expected.

The bearing capacity failure mode may also be affected by the size of the model footing compared with the average particle size of the loaded soil. For relatively large footing, the soil matric suction provides more resistance. However, when the footing size is small, the load applied on the model footing is mostly carried by the individual soil particles and there is significantly less contribution from the frictional resistance between the soil particles (Oh et al., 2009). In this study, since the ratio of footing size (i.e., 100 mm in diameter) to the average soil

particle sizes (i.e., $D_{50} = 0.134$ mm), is approximately 746, a transition in the failure mechanism from punching to local (for soil at relative density of 0%) and from local to general shear failure (for soil at relative density of 40%) are expected at a certain degree of saturation. Table 6 summarizes the interpreted failure modes based on the measured stress-settlement curves.

ANALYSIS BASED ON BEARING CAPACITY EQUATION

Vahedifard and Robinson (2016) presented a model to predict the bearing capacity of unsaturated soils. Their model incorporates the suction stress-based effective stress of Lu et al. (2010) into the general bearing capacity equation of Terzaghi (1943) through the use of a total cohesion concept. It uses the effective saturation as it is used by Lu et al. (2010) to incorporate the parameters of the SWRC into the effective stress relationship. A term referred to as total cohesion is introduced by adding the apparent cohesion (i.e., c_{app}) to the effective cohesion (i.e., $c_{total} = c_{app} + c'$). The total cohesion is then used in Terzaghi's bearing capacity equation to compute the ultimate bearing capacity of unsaturated soils. In this model, the apparent cohesion is defined as the shear strength mobilized by the suction stress, σ^s, through the internal friction angle, ϕ', such that $c_{app} = -\sigma^s \tan\phi'$ (Lu et al., 2009). The bearing capacity is then calculated as follows:

$$q_{ult} = \{c' + (\mathrm{u_a} - \mathrm{u_w})_b(1 - S_{e,AVR})tan\phi' + [(u_a - u_w)S_e]_{AVR}tan\phi'\}N_c\xi_c + q_0N_q\xi_q + 0.5\gamma BN_\gamma\,\xi_\gamma \quad (7)$$

where $(\mathrm{u_a} - \mathrm{u_w})_b$ is the air-entry suction from the SWRC, and $S_{e,AVR}$= the average effective saturation within the stress bulb zone, i.e., 0 to 1.5B, below a shallow foundation, and N_c, N_q, and N_γ are the bearing capacity factors for which N_c and N_q can be determined using the

relationships of Terzaghi (1943). It is noted that in the procedure employed for preparation of the soil in the current study, the profile of the degree of saturation and matric suction with depth beneath the footing is uniform; therefore, the average matric suction of the soil beneath the footing is the same as the matric suction everywhere else in the soil. The value of N_γ proposed by Kumbhojkar (1993) was found to provide better match of the experiments with the predictions (Vanapalli and Mohamed, 2013). The shape factors ξ_c and ξ_γ are calculated using the equations of Vesić (1973) as follows:

$$\xi_c = 1 + (\frac{B}{L})(\frac{N_q}{N_c}) \quad (8)$$

$$\xi_\gamma = 1 - (\frac{B}{L})(\frac{N_q}{N_c}) \quad (9)$$

A comparison of the measured bearing capacity values for the soil with the predicted bearing capacity from the model of Vahedifard and Robinson (2016) for the unsaturated soils at relative densities of 0, 40, 70, and 90% is shown in Figure 8. The interpretation method of Vesic (1963) was used to determine the bearing capacities for the various cases based on the measured stress-settlement curves and where the stress-settlement curves exhibited no peak point. Based on this method, the point of intersection of tangents to the two sections of the stress-settlement curve with larger and smaller slopes was determined, and the stress corresponding to this point was chosen as the bearing capacity. For the curves with an obvious peak point, the stress corresponding to this point was selected as the bearing capacity. Bearing capacities for actual footings are estimated based on either the allowable settlement or the failure load divided by an appropriate factor of safety. In loose soils, failure typically occurs at settlements greater than the allowable value. In the current study, the primary goal is comparing failure loads and their associated settlements for various degrees of saturation and relative densities

rather than the determination or recommendation of allowable or design bearing pressures. Therefore, bearing capacities obtained in the current study for some cases are associated with substantial settlement.

Based on the direct shear test results, the effective cohesion was assumed to be zero. The mobilized friction angle ϕ'_m was determined by modifying the effective friction angle obtained from the direct shear test results to consider dilatancy effects, as follows:

$$\phi'_m = \phi' + \Psi \quad (10)$$

where Ψ is the dilatancy angle. For samples of sand at the same density and similar modes of shearing, a major factor influencing dilation is the stress level at which shearing occurs, such that lower stress levels lead to higher dilatancy (Bolton, 1986). The footing loaded in the tank tests was placed on the soil surface with very low overburden stress acting on the majority of failure surface developed during bearing capacity failure. However, vertical stresses applied in the direct shear tests conducted in this study ranged from 50 to 200 kPa, which are much higher than the aforementioned overburden. Dilatancy would therefore be more suppressed in the direct shear tests and is expected to be higher in the tank tests. An increase in friction angle to account for increase in dilatancy when results of direct shear tests are used in the calculation of bearing capacity of surface footings in test tanks has been applied frequently by researchers in the past (e.g., Steensen-Bach et al. 1987; Oh and Vanapali, 2011; Vanapalli and Mohamed, 2007 and 2013; and Vahedifard and Robinson, 2015). Following recommendation by the Danish Standard (DSCE, 1984) the aforementioned researchers used a 10% increase in friction angle for this purpose, and the same increase is used in the current study. for all relative densities (i.e., $\phi'_m = 1.1\,\phi'$

Values of the parameters used to obtain the predicted bearing capacities for the soil and their corresponding relative densities are presented in Table 6. Where observations indicate that punching or local shear is the likely mode of failure, strength parameters of the soil were reduced by a factor of 1.5 before using them in the bearing capacity equation, as suggested by Terzaghi (1943). A reasonable match is observed between the model predictions and the experimental values in Figure 8, especially when the mode of failure of the soil is better-recognized. Two different predicted capacities for the soil layers at relative densities of 0 and 40% were considered. In the predicted-Local series, it is assumed that the soil experiences local shear, whereas at the predicted-General series, it is assumed that the soil layer experiences general shearing.

DISCUSSION OF RESULTS

Differences between the measured and predicted bearing capacities for the looser soils (i. e., soils at relative densities of 0 and 40%) may result from a number of sources. One of them, especially for tests at initial saturations of 60% or higher (initial degrees of saturation of 60 and 90%) is the type of failure assumed for the determination of the bearing capacity. It can be noticed from the pressure-settlement curves that for soil at these degrees of saturation, no clear peak is observed, and the exact failure mode of the soil is not well known, but it may be considered as a transitional mode between general shear failure and local or punching shear failure. The mode of failure of the soil influences the footing bearing capacity and shape factors used in calculation of the bearing capacity as indicated by Vaseghi et al. (2018). They found that in such cases, the predicted and experimental results match very well when an average of the parameters for the local and general shear failures is used in the model of Vahedifard and

Robinson (2016). Generally, as it can be noticed from Figure 8, the mode of failure for the soil at relative density of 0% and at lower degrees of saturation looks closer to general shear, while this soil experience local shear at higher degrees of saturation. For the soil at relative density of 40%, a clear general shear can be observed at degrees of saturation lower than 30%, however the mode of failure at degrees of saturation higher than 30% seems to be transitional. The other cause of the differences in the measured and calculated bearing capacities may be related to the approximations present in the bearing capacity model proposed by the original researchers (Vahedifard and Robinson, 2016), who also observed some differences between their model predictions and experimental results.

Using the model of Vahedifard and Robinson (2016), a curve showing maximum bearing capacities of the soil for the various conditions (referred to as "Line of Max B.C.") is also presented in Figure 8. In this figure, it was assumed that the soil experiences general shear at its strongest state, as discussed earlier. As can be observed from this figure, increasing the relative density of the soil results in greater values of bearing capacities obtained at lower degrees of saturation. The maximum bearing capacity of a denser soil occurs at a lower degree of saturation. Specifically, for the soil at relative densities of 0 and 90%, maximum values of bearing capacity were obtained at degrees of saturation of 30 and 7%, respectively. Moreover, from Figure 4(b) and Figure 9, a similar trend can be observed in the variations of soil suction stress and bearing capacity, respectively, with the degrees of saturation, but some difference exists in the magnitude of the degrees of saturation at which maximum suction stress and bearing capacity occurs. For a given soil relative density, the maximum bearing capacity occurs at a lower degree of saturation in comparison with that at which the maximum suction stress

occurs. For example, for the soil at relative densities of 0 and 90%, the maximum and minimum values of suction stress were obtained at degrees of saturation of 48 and 18%, respectively, whereas, as mentioned previously, the maximum and minimum values of the bearing capacity occur at degrees of saturation of 30 and 7%, respectively. It should be noted that the maximum suction stress calculated by the Lu et al. (2010) SSCC relationship involves some approximations in the determination of the parameter that is multiplied by the soil suction to obtain the suction stress.

CONCLUSIONS

This study presents an evaluation of the impacts of relative density and degree of saturation on the shear strength and bearing capacity of sands. Results from a series of physical modeling tests involving loading of a circular surface footing on a compacted sand layer demonstrate that changes in bearing capacity with the initial degree of saturation match well with predictions from effective stress models, if appropriate failure modes and their changes from local shear failure to general shear failure are considered. As expected, the bearing capacity was greater for soils with increasing relative density, but an interesting observation is that a transition from general to local shear failure occurred at a certain combination of relative density and degree of saturation. For the silty sand tested, this transition occurred at a relative density of 0% for degrees of saturation between 4 and 16% and at a relative density of 40% for degrees of saturation between 30 and 90%. General shear failure was always observed at relative densities of 70 and 90%.

While direct shear tests showed that increasing soil relative density resulted in increase in friction angle (and, therefore, increase in bearing capacity) for all the degrees of saturation,

as expected, model footing tests showed that decrease in degree of saturation starting from saturated conditions leads to increase in the bearing capacity until a specific degree of saturation is reached. For further decreases in degree of saturation, the bearing capacity decreases in some cases (i.e., for sand layers with relative densities less than 70%) or remains almost constant in other cases (i.e., for very dense soils with a relative density of 90%).

Moreover, the suction stress values inferred from the failure envelopes obtained based on results of the direct shear test were found to match well with values predicted from the soil-water retention curves for sands with various relative densities. Increasing the relative density of the soil resulted in greater bearing capacities, which were obtained at lower degrees of saturation, that is, the maximum bearing capacity of a denser soil occurred at a lower degree of saturation. Moreover, a similar trend was observed in the variation of soil suction stress and bearing capacity with the degrees of saturation, but some differences existed in the magnitude of the degrees of saturation at which maximum suction stress and bearing capacity occurred. For a given soil relative density, the maximum bearing capacity occurred at a lower degree of saturation in comparison with that at which the maximum suction stress occurred. It should be noted that the maximum suction stress calculated by the Lu et al. (2010) SSCC relationship involves some approximations in the determination of the parameter that is multiplied by the soil suction to obtain the suction stress.

References

Birle, E., Heyer, D. and Vogt, N. 2008. “Influence of the initial water content and dry density on the soil–water retention curve and the shrinkage behavior of a compacted clay” Acta Geotechnic.a 3, 191–200. DOI 10.1007/s11440-008-0059-y.

Bolton, M., 1986. The strength and dilatancy of sands. Geotechnique, 36(1): 65-78.

Bolton, M. and Lau, C., 1989. Scale effects in the bearing capacity of granular soils, Proceedings of the 12th International Conference on Soil Mechanics and Foundation Engineering. AA Balkema, pp. 895-898.

Boso, M., 2005. Shear strength behaviour of a reconstituted partially saturated clayey silt, PhD dissertation, Università degli Studi di Trento.

Briaud, J.-L. and Gibbens, R., 1997. Large-scale load tests and data base of spread footings on sand, United States. Federal Highway Administration.

Broms, B.B., 1965. Effect of degree of saturation on bearing capacity of flexible pavements. Highway Research Record(71): 1-14.

Casini, F., Vaunat, J., Romero, E. and Desideri, A., 2012. Consequences on water retention properties of double-porosity features in a compacted silt. Acta Geotechnica, 7(2): 139-150.

Cerato, A.B. and Lutenegger, A.J., 2007. Scale effects of shallow foundation bearing capacity on granular material. Journal of Geotechnical and Geoenvironmental Engineering, 133(10): 1192-1202.

Ciervo, F., Casini, F., Papa, M.N. and Rigon, R., 2015. Some remarks on bimodality effects of the hydraulic properties on shear strength of unsaturated soils. Vadose Zone Journal, 14(9).

Colliat-Dangus, J.L., Desrues, J. and Foray, P., 1988. Triaxial testing of granular soil under elevated cell pressure, Advanced triaxial testing of soil and rock. ASTM International, pp. 290- 310.

Costa, Y.D., Cintra, J.C. and Zornberg, J.G., 2003. Influence of matric suction on the results of plate load tests performed on a lateritic soil deposit. Geotechnical Testing Journal, 26(2): 219-227.

DSCE. 1984. The Danish Code of Practice for Foundation Engineering. Danish Standard DS 415. Danish Society of Civil Engineering (DSCE), Copenhagen, Denmark.Fredlund, D.G. and Rahardjo, H., 1993. Soil Mechanics for Unsaturated Soils. John Wiley & Sons, 517 pp.

Gens, A., Sánchez, M. and Sheng, D., 2006. On constitutive modelling of unsaturated soils. Acta Geotechnica, 1(3): 137-147.

Ghaaowd, I., McCartney, J.S., Thielmann, S.S., Sanders, M.J. and Fox, P.J., 2017. Shearing behavior of tire-derived aggregate with large particle size. I: Internal and concrete interface direct shear. Journal of Geotechnical and Geoenvironmental Engineering, 143(10): 04017078.

Herle, I., 1997. Effect of grain size and pressure level on bearing capacity of footings on sand. Deformation and Progressive Failure in Geomechanics: 781-786.

Hettler, A. and Gudehus, G., 1988. Influence of the foundation width on the bearing capacity factor. Soils and Foundations, 28(4): 81-92.

Imam, R., Vaseghi Maghvan, S. and McCartney, J.S., 2018. “Shear strength of unsaturated sand at different relative densities.” 7th International Conference on Unsaturated Soils (UNSAT2018). C.W.W. Ng, A.K. Leung, A.C.F. Chiu, C. Zhou, eds. The Hong Kong University of Science and Technology. 191-196.Kumbhojkar, A., 1993. Numerical evaluation of Terzaghi's N γ. Journal of Geotechnical Engineering, 119(3): 598-607.

Kusakabe, O., 1995. Foundations. Geotechnical centrifuge technology, R. N. Taylor, ed.: Blackie Academic & Professional, London: 118-167.

Lambe, T. W. and Whitman, R. W., 1979, Soil Mechanics, John Wiley and Sons, New York, pp. 553.Lau, C. and Bolton, M., 2011. The bearing capacity of footings on granular soils. II: Experimental evidence. Géotechnique, 61(8): 639-650.

Loukidis, D. and Salgado, R., 2011. Effect of relative density and stress level on the bearing capacity of footings on sand. Géotechnique, 61(2): 107-119.

Lu, N., Godt, J.W. and Wu, D.T., 2010. A closed-form equation for effective stress in unsaturated soil. Water Resources Research, 46(5): 14.

Lu, N. and Likos, W.J., 2004. Unsaturated soil mechanics. Jhon Wiley, New York, 556 pp.

Miller, G. and Muraleetharan, K., 1998. In situ testing in unsaturated soil, Proceedings of the Second International Conference on Unsaturated Soils, Beijing, China, pp. 416-421.

Mitchell, J.K., Hooper, D.R., and Campanella, R.G., 1965. Permeability of compacted clay. J. Soil. Mech. Found. Div. 91 (SM4), 41–65.

Mohamed, F. and Vanapalli, S., 2006. Laboratory investigations for the measurement of the bearing capacity of an unsaturated coarse-grained soil, Proceedings of the 59th Canadian Geotechnical Conference, Vancouver, BC, pp. 1-4.

Oh, W.T. and Vanapalli, S.K., 2011. Modelling the applied vertical stress and settlement relationship of shallow foundations in saturated and unsaturated sands. Canadian Geotechnical Journal, 48(3): 425-438.

Oh, W.T. and Vanapalli, S.K., 2013. Scale effect of plate load tests in unsaturated soils. Int. J. Geomater, 4(2): 585-594.

Oh, W.T., Vanapalli, S.K. and Puppala, A.J., 2009. Semi-empirical model for the prediction of modulus of elasticity for unsaturated soils. Canadian Geotechnical Journal, 46(8): 903-914.

Oloo, S.Y., Fredlund, D. and Gan, J.K., 1997. Bearing capacity of unpaved roads. Canadian Geotechnical Journal, 34(3): 398-407.

Palmer, L., 1948. Field Loading Tests for the Evaluation of the Wheel-Load Capacities of Airport Pavements, Symposium on Load Tests of Bearing Capacity of Soils. ASTM International, pp. 9-30.

Perkins, S.W. and Madson, C.R., 2000. Bearing capacity of shallow foundations on sand: A relative density approach. Journal of Geotechnical and Geoenvironmental Engineering, 126(6): 521-530.

Schnaid, F., Consoli, N., Cudmani, R. and Militistsky, J., 1995. Load-settlement response of shallow foundations in structured unsaturated soils, Proceedings of the First International Conference of Unsaturated Soils, Paris, France, pp. 999-1004.

Simonini, P., 1993. Influence of relative density and stress level on the bearing capacity of sands. International Journal for Numerical and Analytical Methods in Geomechanics, 17(12): 871-890.

Sheng, D., Sloan, S.W., Gens, A. and Smith, D.W., 2003. Finite element formulation and algorithms for unsaturated soils. Part I: Theory. International Journal for Numerical and Analytical Methods in Geomechanics, 27(9): 745-765.

Steensen-Bach, J., Foged, N. and Steenfelt, J., 1987. Capillary induced stresses—fact or fiction?, European Conference on Soil Mechanics and Foundation Engineering. 9, pp. 83-89.

Tang, Y., Taiebat, H.A. and Russell, A.R., 2016. Bearing capacity of shallow foundations in unsaturated soil considering hydraulic hysteresis and three drainage conditions. International Journal of Geomechanics, 17(6): 040161421-0401614213.

Tatsuoka, F., 1991. Progressive failure and particle size effect in bearing capacity of a footing on sand, Proc. of Geotech. Eng. Congress, Special Publication, ASCE, pp. 788-802.

Terzaghi, K., 1943. Theoretical Soil Mechanics. John Wiley and Sons, New York, NY, USA.

Toll, D.G., 1990. A framework for unsaturated soil behaviour. *Géotechnique*, *40*(1), pp.31-44.

Toll, D.G. and Ong, B.H., 2003. Critical-state parameters for an unsaturated residual sandy clay. *Géotechnique.*, *53*(1), pp.93-103.

Uchaipichat, A., 2010. Prediction of shear strength for unsaturated soils under drying and wetting processes. Electronic Journal of Geotechnical Engineering, 15: 1087-1102.

Vahedifard, F. and Robinson, J.D., 2016. Unified method for estimating the ultimate bearing capacity of shallow foundations in variably saturated soils under steady flow. Journal of Geotechnical and Geoenvironmental Engineering, 142(4): 04015095.

van Genuchten, M.T., 1980. A closed-form equation for predicting the hydraulic conductivity of unsaturated soils. Soil Science Society of America Journal, 44(5): 892-898.

Vanapalli, S.K. and Mohamed, F.M., 2007. Bearing capacity of model footings in unsaturated soils. Experimental Unsaturated Soil Mechanics. Springer-Verlag, Berlin Heidelberg, Germany: 483-493.

Vanapalli, S.K. and Mohamed, F.M., 2013. Bearing capacity and settlement of footings in unsaturated sands. Int. J. of GEOMATE, 5(1): 595-604.

Vaseghi Maghvan, S., Imam, R., and McCartney, J.S., 2018. Physical modeling of stone columns in unsaturated soil deposits. Geotechnical Testing Journal. https://doi.org/10.1520/GTJ20170405.

Vesić, A.S., 1973. Analysis of ultimate loads of shallow foundations. Journal of the Soil Mechanics and Foundations Division, 99(1): 45-73.

Wood, F. M., Yamamuro, J. A. and Lade, P. V. 2008. Effect of depositional method on the undrained response of silty sand. Canadian Geotechnical Journal. 45. pp. 1525-1537.

Yamaguchi, H., Kimura, T. and Fuji, N., 1976. On the influence of progressive failure on the bearing capacity of shallow foundations in dense sand. Soils and Foundations, 16(4): 11-22.

Zhao, H., Zhang, L. and Chang, D., 2012. Behavior of coarse widely graded soils under low confining pressures. Journal of Geotechnical and Geoenvironmental Engineering, 139(1): 35-48.

Zhu, F., Clark, J.I. and Phillips, R., 2001. Scale effect of strip and circular footings resting on dense sand. Journal of Geotechnical and Geoenvironmental Engineering, 127(7): 613-621.

Table

Table 1- Geotechnical properties of the silty sand.

Property	**Silty Sand**
D_{10} (mm)	0.081
D_{30} (mm)	0.105
D_{50} (mm)	0.135
D_{60} (mm)	0.161
Specific gravity, G_s	2.64
Maximum dry unit weight, $\gamma_{d(max)}$ (kN/m^3)	15.5
Minimum void ratio, e_{min}	0.68
Minimum dry unit weight, $\gamma_{d(min)}$ (kN/m^3)	13.6
Maximum void ratio, e_{max}	0.90
Coefficient of curvature, C_z	0.85
Coefficient of uniformity, C_u	1.99
Fines content (<0.075 mm, %)	7.0

Table 2- Summary of initial conditions for the silty sand at four different initial relative densities.

Relative Density, D_r (%)	Dry unit weight (kN/m^3)	Void ratio, e	Effective cohesion, c′ (kPa)
0	13.6	0.90	0
40	14.3	0.81	0
70	14.6	0.77	0
90	15.25	0.70	0

Table 3. Friction angle and apparent cohesion values obtained from the direct shear tests on silty sand specimens having different initial degrees of saturation at four different relative densities.

Initial degree of saturation, S_r (%)	Relative density, D_r (%)											
	0			40			70			90		
	c_{app} (kPa)	Drained Friction Angle, ϕ′ (°)	R^2	c_{app} (kPa)	Drained Friction Angle, ϕ′ (°)	R^2	c_{app} (kPa)	Drained Friction Angle, ϕ′ (°)	R^2	c_{app} (kPa)	Drained Friction Angle, ϕ′ (°)	R^2
0	0.00	31.0	0.98	0.00	32.6	0.99	0.00	34.5	0.98	0.00	36.3	0.98
4	1.07		0.99	1.21		0.99	3.77		0.98	5.00		0.99
16	1.17		0.98	2.05		0.99	3.54		0.98	4.96		0.99
30	1.32		0.99	1.91		0.99	2.96		0.99	4.22		0.99
60	1.20		0.98	1.71		0.99	2.27		0.98	3.10		0.99
90	0.65		0.99	0.89		0.99	1.12		0.98	1.55		0.98
100	0.00		0.99	0.00		0.99	0.00		0.99	0.00		0.96

Table 4. SWRCs parameters for the silty sand at different relative densities [After Imam et al., 2018].

	Relative density, D_r (%)			
Parameter	0	40	70	90
AEV (kPa)	1.44	1.67	2.27	2.92
S_{res} (%)	0.00	0.00	0.00	0.00
α_{vG} (kPa^{-1})	0.34	0.28	0.20	0.16
n_{vG}	2.40	2.14	2.08	2.04

Table 5. Values of the measured bearing capacity (B.C.) and corresponding footing settlements for tests on silty sand layers having different initial degrees of saturation and relative densities.

S_r (%	Relative density, D_r (%)							
	0		40		70		90	
	B.C. (kPa)	Settlement (mm)	B.C. (kPa)	Settlement (mm)	B.C. (kPa)	Settlement (mm)	B.C. (kPa)	Settlement (mm)
0	45	16	197	25	-	-	-	-
4	70	10	259	15	548	4.5	1250	5.0
16	125	16	330	20	539	6.4	957	6.5
30	157	9	245	43	-	-	-	-
60	75	11	137	9	336	7.1	738	7.0
90	40	13	107	10	-	-	-	-

Table 6- Parameters used in the bearing capacity predictions for the silty sand layers.

Relative density, D_r (%)	Drained friction angle, ϕ' (°)	ϕ'_m (°)	Drained cohesion, c' (kPa)	Failure mode	N_c	N_q	N_γ	ξ_c	ξ_γ
0	31.0	34.0	0	Local	24.0	13.0	9.0	1.54	0.6
				General	50.0	36.0	39.0	1.72	
40	32.6	35.8		Local	27.0	14.0	6.0	1.52	
				General	58.0	44.4	49.7	1.76	
70	34.5	38.0		General	72.0	70.0	78.6	1.97	
90	36.3	39.9		General	93.0	97.0	112.0	2.04	

Figure

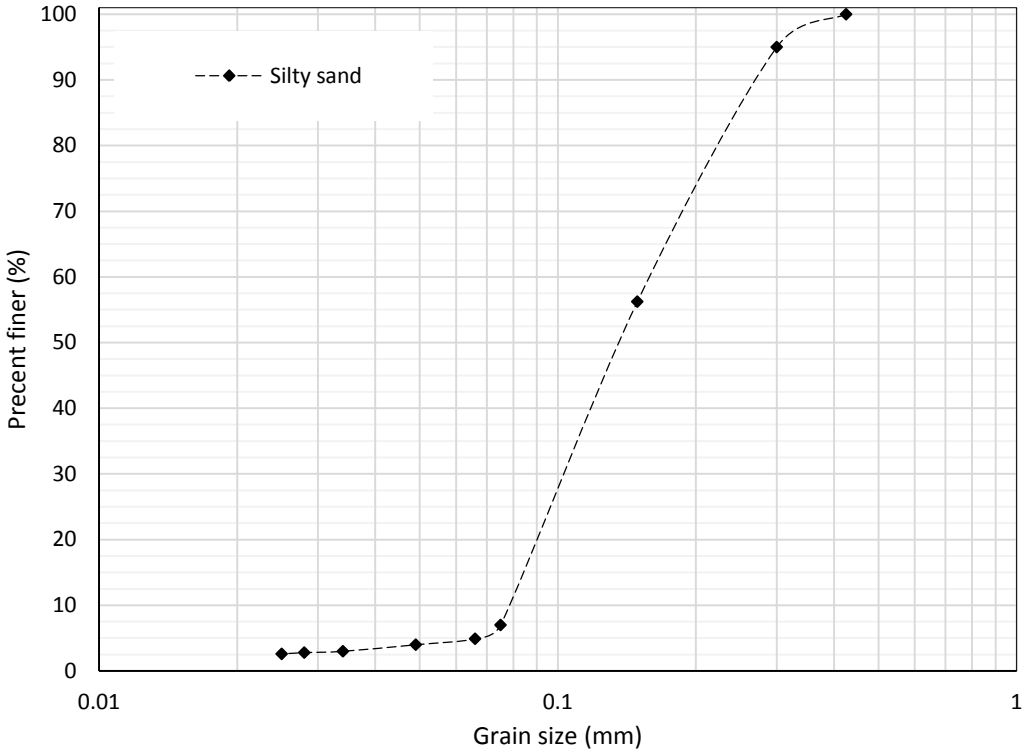

Figure 1- Grain size distribution for the silty sand.

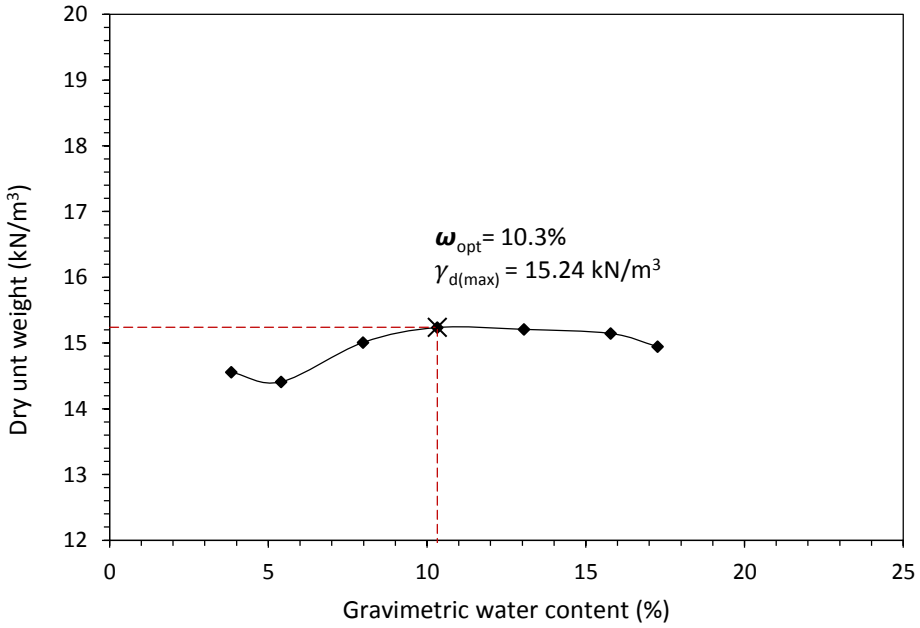

Figure 1- Compaction curve for the silty sand.

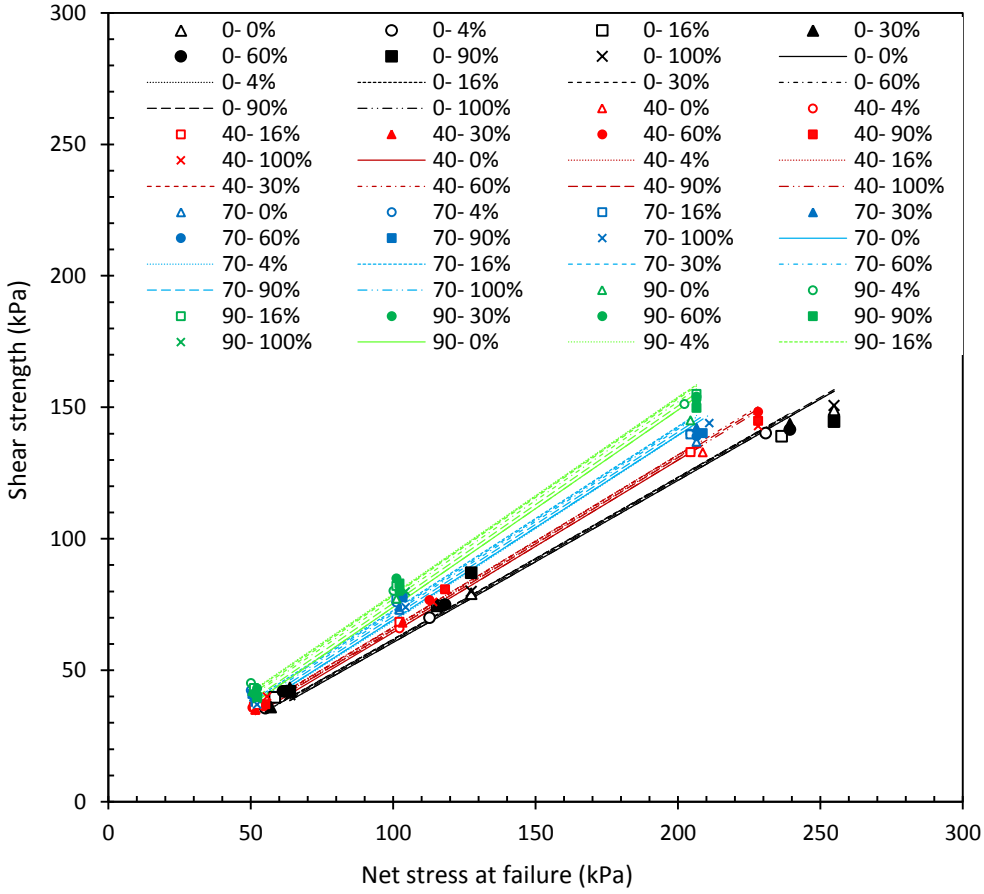
0- 0%
0- 4%
0- 16%
0- 30%
0- 60%
0- 90%
0- 100%
0- 0%
0- 4%
0- 16%
0- 30%
0- 60%
0- 90%
0- 100%
40- 0%
40- 4%
40- 16%
40- 30%
40- 60%
40- 90%
40- 100%
40- 0%
40- 4%
40- 16%
40- 30%
40- 60%
40- 90%
40- 100%
70- 0%
70- 4%
70- 16%
70- 30%
70- 60%
70- 90%
70- 100%
70- 0%
70- 4%
70- 16%
70- 30%
70- 60%
70- 90%
70- 100%
90- 0%
90- 4%
90- 16%
90- 30%
90- 60%
90- 90%
90- 100%
90- 0%
90- 4%
90- 16%
Shear strength (kPa)
Net stress at failure (kPa)
0
50
100
150
200
250
300

(a)

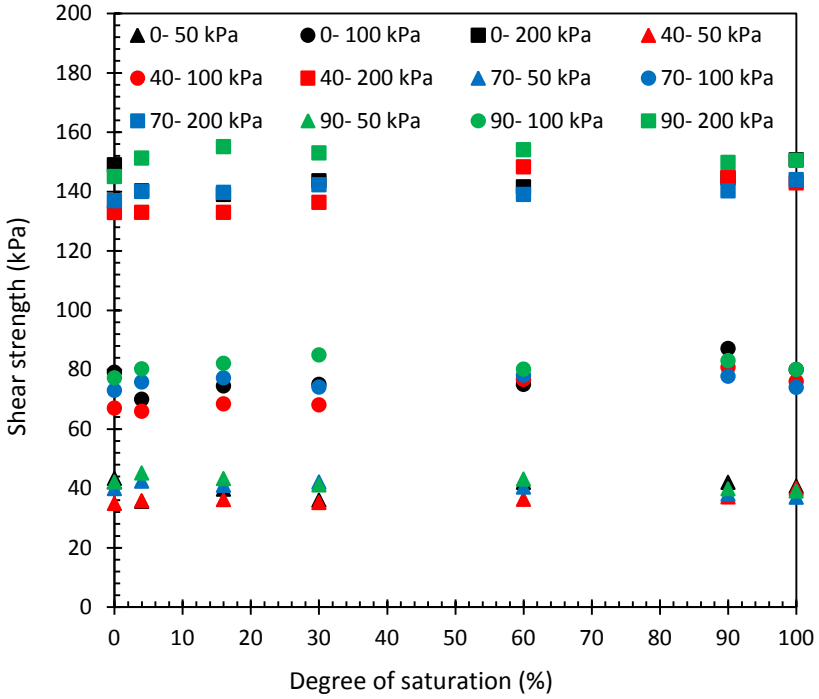
0- 50 kPa
0- 100 kPa
0- 200 kPa
40- 50 kPa
40- 100 kPa
40- 200 kPa
70- 50 kPa
70- 100 kPa
70- 200 kPa
90- 50 kPa
90- 100 kPa
90- 200 kPa
Shear strength (kPa)
Degree of saturation (%)
0
20
40
60
80
100
120
140
160
180
200
0
10
20
30
40
50
60
70
80
90
100

(b)

Figure 3- (a) Failure envelopes (obtained from the shear stress values corresponding to the maximum mobilized secant friction angles) in terms of net vertical stress for the silty sand under different initial degrees of saturation at relative densities of: 0% (black lines); 40% (red lines); 70% (blue lines); and 90% (green lines) ; (b) Variation of shear strength of the silty sand with degree of saturation for different initial vertical net stresses of 50, 100, and 200 kPa at relative densities of 0%; 40%; 70%; and 90%. (Note: Numbers in legend are from left to right are relative density and vertical net stresses). [After Imam et al. (2018)].

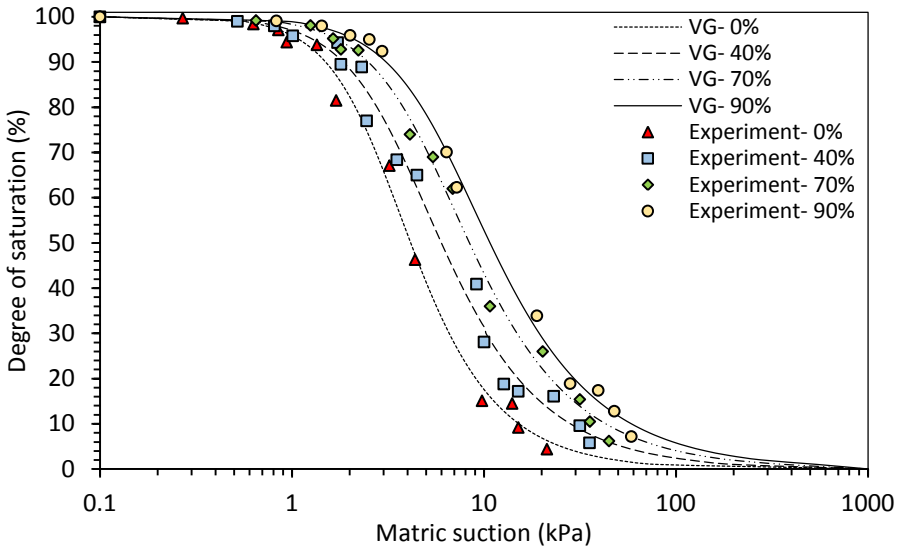

(a)

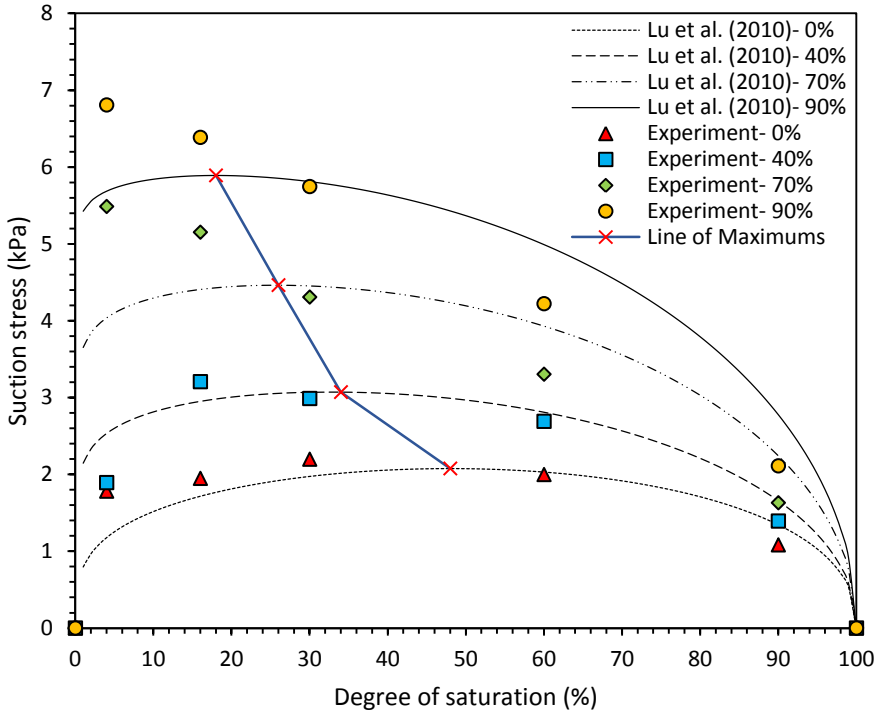

(b)

Figure 4- (a) SWRC data for sand at different relative densities fitted with the van Genuchten (1980) model; (b) Suction stress characteristic curves predicted from the SWRCs for the silty sand under different relative densities along with data points inferred from the failure envelopes.

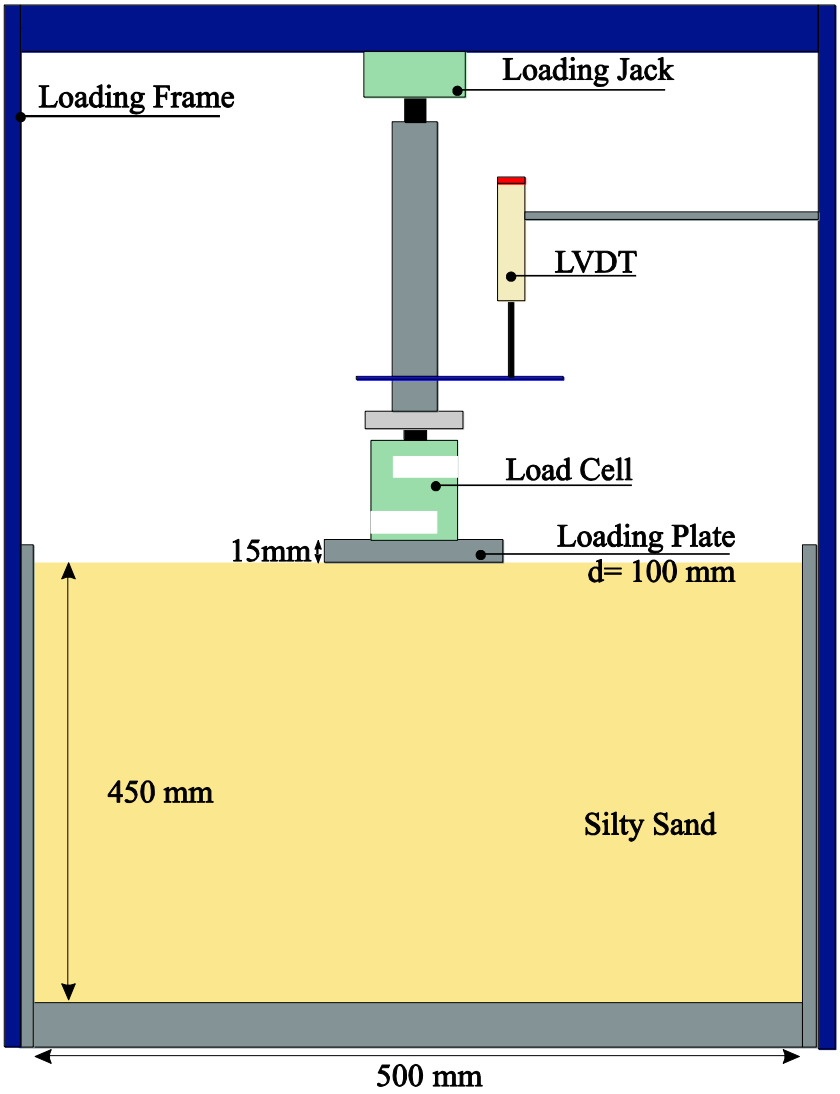

Figure 5- Details of the experimental setup for characterization of the axial loading response of unsaturated silty sand layers.

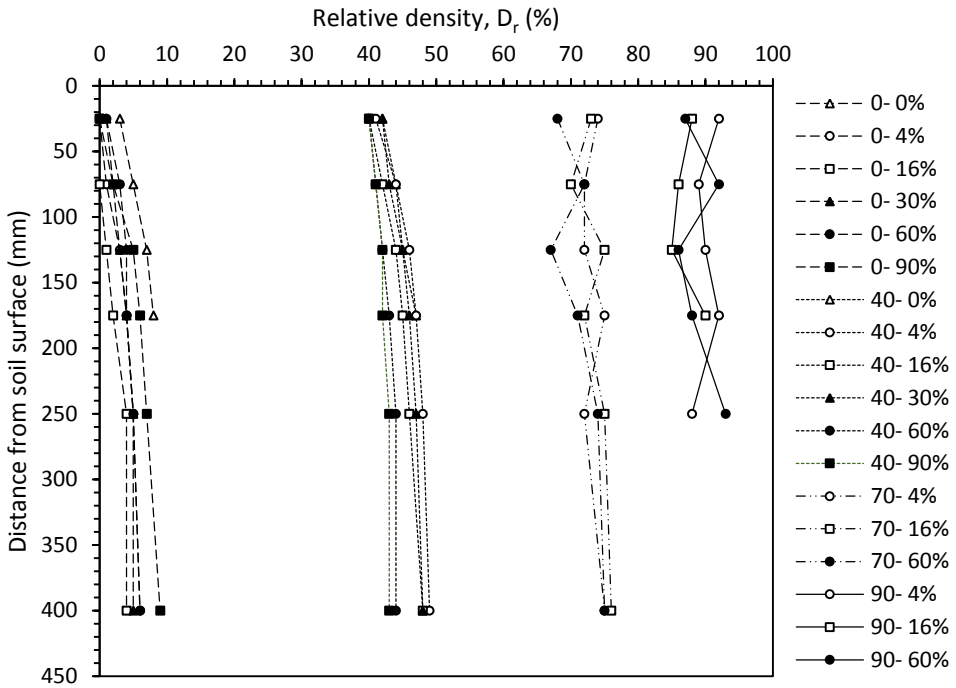

Figure 6- Variations of soil relative density after constructing the soil layers at various initial degrees of saturation [numbers in legend from left to right are: Relative density (%) and initial degree of saturation].

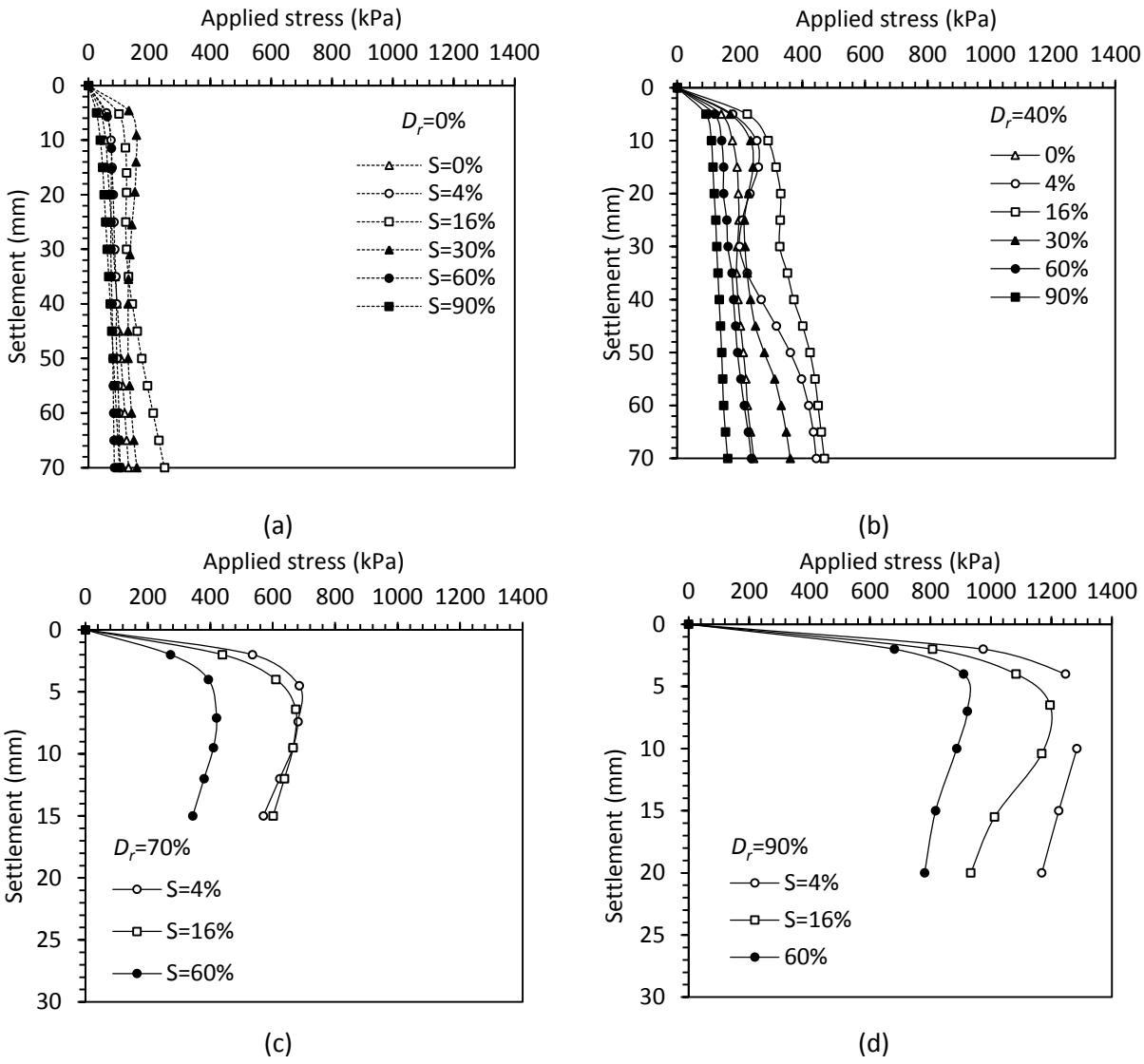

Figure 7- Relationships between the applied footing stresses versus footing settlements for the silty sand layers compacted to different initial degrees of saturation and relative densities of: (a) 0%; (b) 40%; (c) 70%; (d) 90%. (Note: Capacity of load cell exceeded in test on D_r=90%, S=4%)

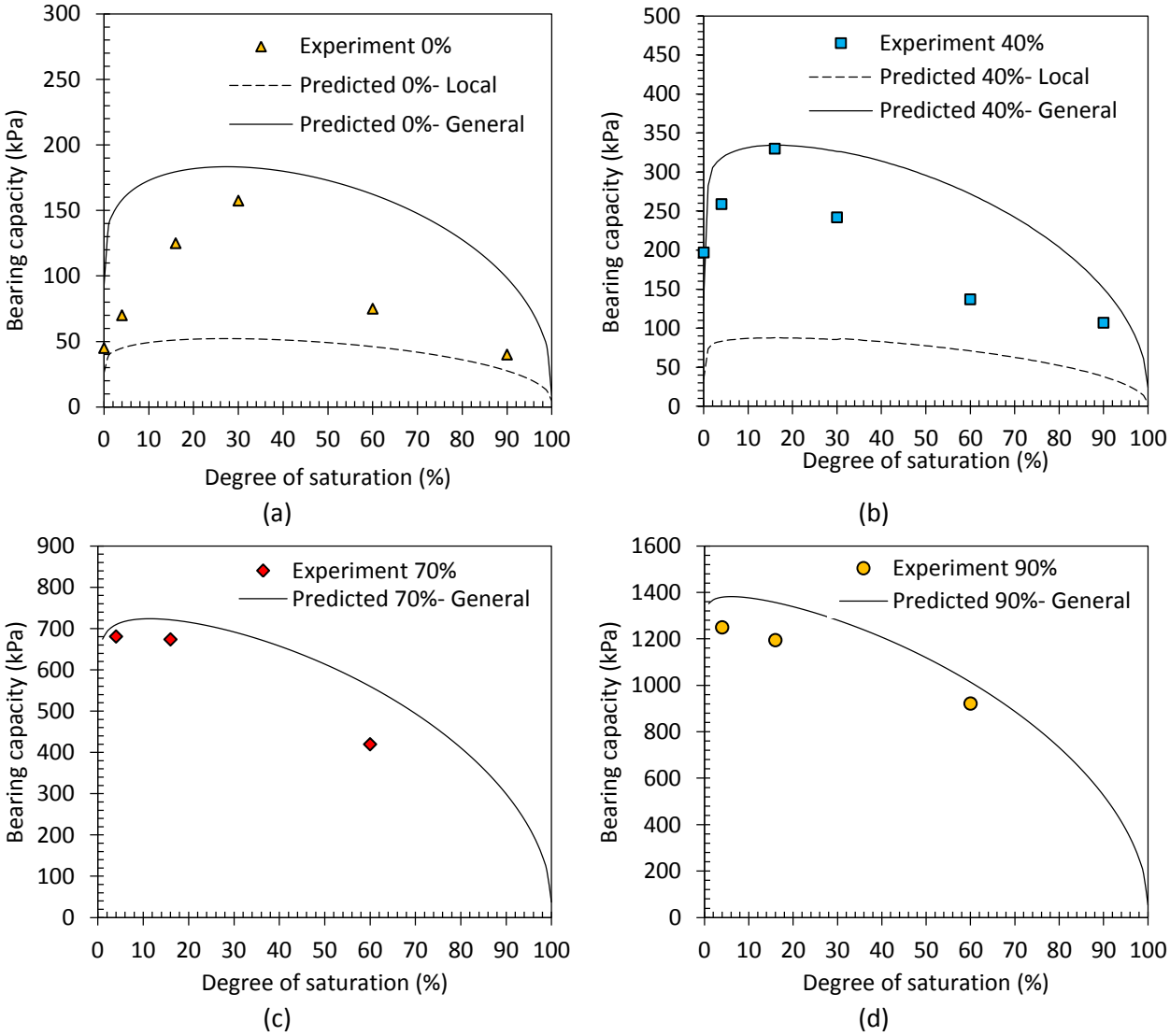

Figure 8- Comparison of experimentally measured and predicted bearing capacity for the unsaturated silty sand layers at relative densities of: (a) 0%; (b) 40%; (c) 70%; (d) 90%. (Note: the failure mode for each case is indicated in Table 6).

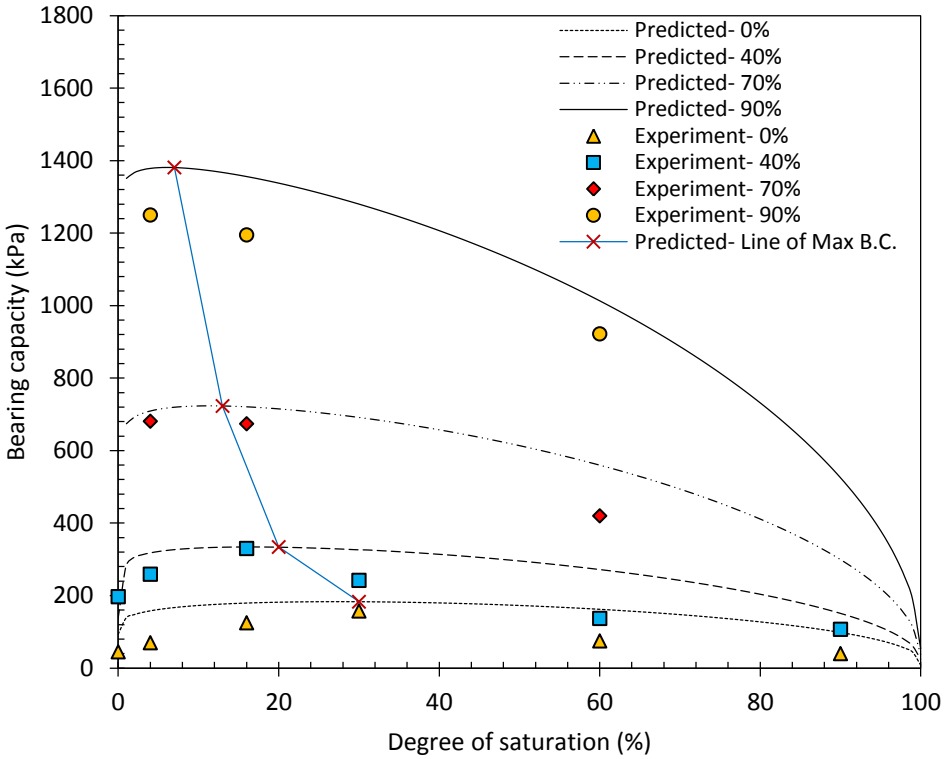

Figure 9- Comparison of experimentally-measured and predicted bearing capacity values for footings on unsaturated silty sand layers having different relative densities.